

REPORT DOCUMENTATION PAGE

Form Approved
OMB No. 0704-0188

The public reporting burden for this collection of information is estimated to average 1 hour per response, including the time for reviewing instructions, searching existing data sources, gathering and maintaining the data needed, and completing and reviewing the collection of information. Send comments regarding this burden estimate or any other aspect of this collection of information, including suggestions for reducing the burden, to Department of Defense, Washington Headquarters Services, Directorate for Information Operations and Reports (0704-0188), 1215 Jefferson Davis Highway, Suite 1204, Arlington, VA 22202-4302. Respondents should be aware that notwithstanding any other provision of law, no person shall be subject to any penalty for failing to comply with a collection of information if it does not display a currently valid OMB control number.
PLEASE DO NOT RETURN YOUR FORM TO THE ABOVE ADDRESS.

1. REPORT DATE (DD-MM-YYYY) 03/30/2015		2. REPORT TYPE Quarterly progress report		3. DATES COVERED (From - To) 12-15-2014 to 04-03-2015	
4. TITLE AND SUBTITLE Noise of High-Performance Aircraft at Afterburner				5a. CONTRACT NUMBER	
				5b. GRANT NUMBER N00014-15-1-2008	
				5c. PROGRAM ELEMENT NUMBER	
6. AUTHOR(S) Tam, Christopher				5d. PROJECT NUMBER	
				5e. TASK NUMBER	
				5f. WORK UNIT NUMBER	
7. PERFORMING ORGANIZATION NAME(S) AND ADDRESS(ES) Sponsored Research Administration Florida State University 874 Traditions Way Tallahassee, FL 32306-4166				8. PERFORMING ORGANIZATION REPORT NUMBER 035259	
9. SPONSORING/MONITORING AGENCY NAME(S) AND ADDRESS(ES) Office of Naval Research AEROSPACE SCIENCE RESEARCH DIV 875 N. Randolph Street Arlington VA 22203-1995				10. SPONSOR/MONITOR'S ACRONYM(S) ONR	
				11. SPONSOR/MONITOR'S REPORT NUMBER(S)	
12. DISTRIBUTION/AVAILABILITY STATEMENT DISTRIBUTION STATEMENT A: Approved for public release: distribution unlimited.					
13. SUPPLEMENTARY NOTES					
14. ABSTRACT The main objective of this project is to obtain a fundamental understanding of the physics of noise generation of a high-performance aircraft operating at afterburner condition. The new noise components are indirect combustion noise produced by the passage of entropy waves through the nozzle of the jet. To obtain a good understanding of the noise generation processes through numerical simulation, it is imperative that a way be found to reproduce such a random wave field with prescribed statistical averaged properties computationally. Here the development of a one-dimensional computational model capable of generating a broadband entropy wave field with a prescribed intensity and frequency spectrum is reported					
15. SUBJECT TERMS Jet noise at afterburner					
16. SECURITY CLASSIFICATION OF:			17. LIMITATION OF ABSTRACT	18. NUMBER OF PAGES	19a. NAME OF RESPONSIBLE PERSON
a. REPORT	b. ABSTRACT	c. THIS PAGE			Christopher Tam
U	U	U	UU	10	19b. TELEPHONE NUMBER (Include area code) 850-644-2455

Quarterly Progress Report

This report covers the period of December 15, 2014 to March 14, 2015

Submitted to

The Office of Naval Research

Project Title : Noise of High-Performance Aircraft at Afterburner

Principal Investigator

Dr. Christopher Tam

Department of Mathematics

Florida State University

Email: tam@math.fsu.edu

Grant Monitor

Dr. John Spyropoulos

Email: John.Spyropoulos@jsf.mil

Technical Representative

Dr. Joseph Doychak

Email: joseph.doychak@navy.mil

20150414073

Summary

The main objective of this project is to obtain a fundamental understanding of the physics involved in the generation of two new noise components (new relative to the noise of standard laboratory hot supersonic jets) when a high-performance aircraft is operating at afterburner condition. It has been proposed (Tam and Parrish "Noise of high-performance aircraft at afterburner" AIAA Paper 2014-2754) that the new noise components are indirect combustion noise produced by the passage of entropy waves through the velocity gradients inside the nozzle of the jet. The entropy waves are hot spots created in the combustor and afterburner by the combustion process. The hot spots form a random broadband field. The hot spots are convected downstream by the mean flow. To obtain a good understanding of the noise generation processes through numerical simulation, it is imperative that a way be found to reproduce such a random wave field with prescribed statistical averaged properties computationally. This random wave field forms the input to any numerical simulation study of indirect combustion noise generation. Producing a three dimensional random entropy wave field has not been done before. It is a major challenge to this project. Since there is nothing in the literature, it is believed that it would be useful to concentrate first on the development of a one dimensional computational model capable of generating a broadband entropy wave field with a prescribed intensity and frequency spectrum. This is the primary task of the first quarter of this project. We would like to report that we have accomplished this task. Details of the stochastic model/boundary condition and numerical results are reported below.

1. Stochastic entropy wave model as a CAA inflow boundary condition.

Figure 1 shows a random entropy wave field consisting hot and cold spots convecting downstream through a military-styled convergent-divergent supersonic nozzle by the mean flow. According to indirect combustion noise theory, sound is generated as the entropy waves field passes through the region with large velocity gradient, especially near the nozzle throat. To simulate the noise generation processes, the use of a finite computational domain is inevitable. A reasonable choice is to restrict the computational domain to what is shown in figure 1. With this choice, the inflow boundary is at the left boundary of figure 1. In other words, there is an incoming random broadband entropy wave field at the left boundary. This, therefore, requires that the boundary condition imposed on the left boundary to take on the task of generating the random entropy wave field. In other words, the development of a CAA inflow model boundary condition capable of producing a random entropy waves is required. This CAA boundary condition will be used in the simulation effort of this project.

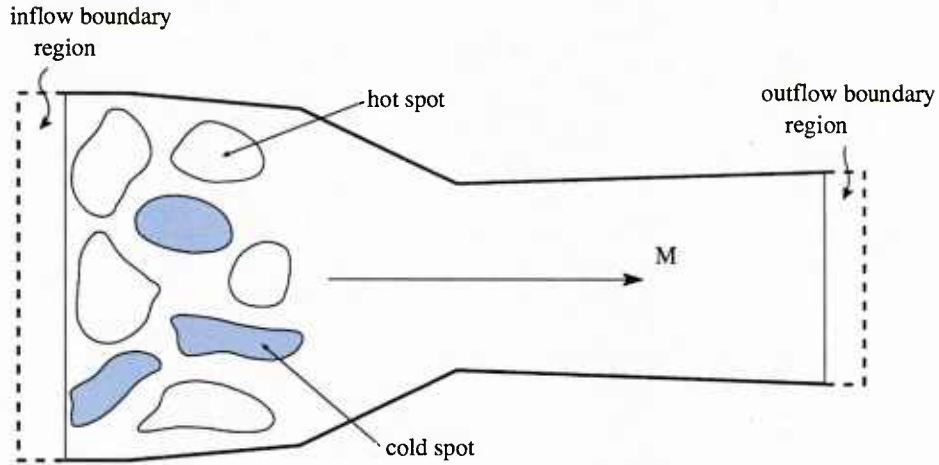


Figure 1. A computational domain for the investigation of the generation of indirect combustion noise inside a military-styled convergent-divergent nozzle.

2. Stochastic properties of a broadband entropy wave field.

In a jet engine, the entropy blobs are of different sizes and shape. So the field of entropy blobs can only be described in statistical terms. One would like to be able to impose a set of statistical properties such as intensity of temperature fluctuation, its spectrum and the size distribution of the entropy blobs. Our intent is to impose the following most relevant physical quantities involving single-point statistics and two-point statistics.

a. Single-point statistics

i. Intensity of temperature fluctuations, $\overline{T'^2}$ where T' is the temperature fluctuations

ii. Frequency spectrum, $S(\omega)$

$$S(\omega) = \frac{1}{2\pi} \int_{-\infty}^{\infty} \overline{T'(t)T'(t+\tau)} e^{-i\omega\tau} d\tau$$

Note: Frequency spectrum is the Fourier transform of the autocorrelation function. In the above, an overbar denotes a time average. Variables with a prime imply fluctuation quantities.

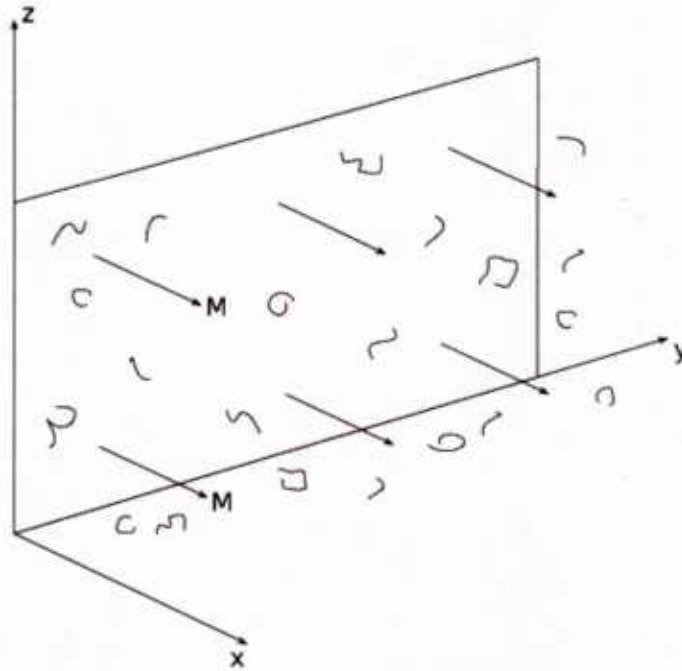


Figure 2. Random entropy disturbances convected downstream in the x-direction by the mean flow pass through a lateral y-z plane. Disturbances on the y-z plane are stochastic. They differ from point to point and from one time to another. However the single-point statistics, $\overline{T'^2}$ and $S(\omega)$ are the same at all points i.e. the stochastic field is spatially homogeneous.

Figure 2 illustrates the significance of single-point statistics in a stochastic field of disturbances. In this figure, the x – axis is the direction of mean flow. The y - z plane is normal to the flow. The entropy blobs on the y – z plane are randomly distributed at any instant of time. However, for any point on this plane, the single-point statistics, $\overline{T'^2}$ and $S(\omega)$ are the same everywhere although T' is spatially and temporally random and stochastic.

b. Two-point statistics

- iii. Two-point correlation function in the y-direction.
- iv. Two-point correlation function in the z-direction.

The sizes of incoming entropy blobs is a quantity one would like to be able to impose on a numerical simulation. Statistically, this can be done by specifying that the incoming stochastic entropy wave field has a prescribed two-point spatial correlation function. In other words, information on blob size distribution is encoded in the two-point spatial correlation function. A two-point correlation function with a narrow half-width

means that the blobs are small in size whereas a broad two-point correlation function means large blobs. Figure 3 shows a bell-shaped two-point correlation function in the y-direction. Naturally, entropy blobs are three-dimensional. So, there is also a two-point correlation function in the z-direction. Statistically, if there is no preferred direction, then the correlation function in the y and z directions would be the same. In developing the stochastic model boundary condition, we plan to allow the user the option to have non-equal correlation function in the y and z direction. This will mean that the wave field is anisotropic.

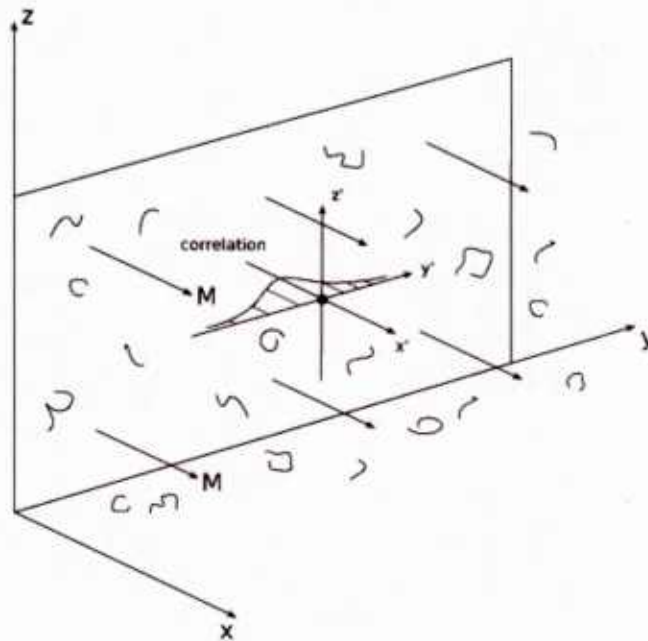


Figure 3. Two-point spatial correlation function in the y-direction for a point in a stochastic field of entropy blobs.

3. A one-dimensional stochastic time-domain entropy wave source model/boundary condition

Let Δx be the mesh spacing
 λ be the size of the dominant entropy wave blob

Dimensionless variables will be used. Let

λ be the length scale
 a_0 (the speed of sound of the mean flow) be the velocity scale
 λ/a_0 be the time scale

ρ_0 (the density of the mean flow) be the density scale
 $\rho_0 a_0^2$ be the pressure scale

For linearized disturbances of a one-dimensional compressible flow associated with a uniform mean flow of Mach number M , the governing equations are the linearized Euler equations. In dimensionless form, they are:

$$\frac{\partial T}{\partial t} + M \frac{\partial T}{\partial x} + (\gamma - 1) \bar{T} \frac{\partial u}{\partial x} = 0 \quad (1)$$

$$\frac{\partial u}{\partial t} + M \frac{\partial u}{\partial x} + \frac{\bar{T}}{\gamma \bar{p}} \frac{\partial p}{\partial x} = 0 \quad (2)$$

$$\frac{\partial p}{\partial t} + M \frac{\partial p}{\partial x} + \gamma \bar{p} \frac{\partial u}{\partial x} = 0 \quad (3)$$

We propose the following broadband entropy wave generation model/boundary condition in one-dimension.

$$T = \sum_{j=1}^N A_j \cos \left[\omega_j \left(\frac{x}{M} - t \right) + \phi_j \right] \quad (4)$$

$$u = 0 \quad (5)$$

$$p = 0 \quad (6)$$

where $\frac{1}{2} A_j^2 = 2S(\omega_j) \Delta \omega_j \quad (7)$

$S(\omega)$ is the prescribed entropy wave spectrum, ϕ_j is a random number between 0 and 2π . It is easy to show that (4), (5) and (6) is a solution to the governing equations (1) to (3).

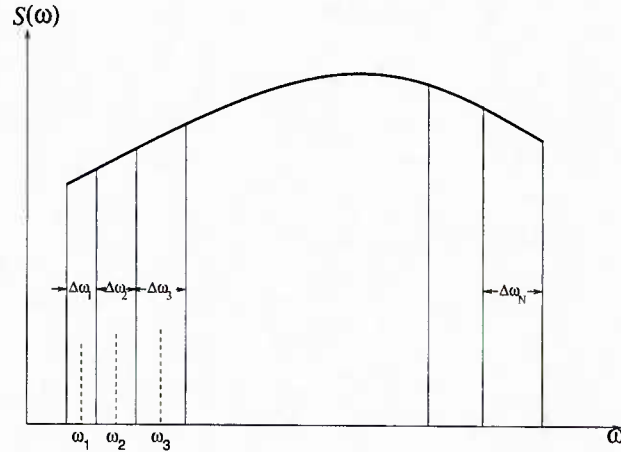


Figure 4. Energy conserving discretization of a prescribed entropy wave spectrum.

For a given wave spectrum $S(\omega)$ as shown in figure 4, in order to form a temperature fluctuating temperature field, the spectrum is first discretized into narrow bands with a center frequency of ω_j ($j=1, 2, 3, \dots$). Each band forms a time harmonic entropy wave with a random phase ϕ_j (see equation (4)). Since entropy waves are convected downstream by the mean flow, all entropy waves are convected downstream at the same Mach number M . To conserve energy, the amplitude A_j of the j^{th} wave is given by equation (7). In (7) the left side is the energy of an oscillator with amplitude A_j . The right side of (7) is the energy of the same oscillator as given by the prescribed spectrum. The two must be equal if energy is conserved in the discretization. On starting with equation (4), it is straightforward to show that the random temperature field has a spectrum equal to $S(\omega)$.

4. Numerical results

As a test case, we consider an entropy wave field with the following Gaussian spectrum

$$S(\omega) = e^{-\ln(2)\left[\frac{\omega-\omega_0}{b}\right]^2} + e^{-\ln(2)\left[\frac{\omega+\omega_0}{b}\right]^2} \quad (8)$$

The values of the parameters of the model are chosen to be,

$$M = 0.3, \quad \omega_0 = 1.885, \quad b = 0.5\omega_0$$

To implement the model boundary condition, the prescribed spectrum is first divided into 500 equally spaced bands. The spectrum is truncated at a frequency of ω_{\max} . For this model, various other parameters are assigned the values below,

$$\omega_{\max} = 3 \omega_0, \quad N = 500, \quad \Delta\omega = \omega_{\max} / N$$

This gives the location of the band center frequencies to be,

$$\omega_j = (j-0.5)\Delta\omega, \quad 1 \leq j \leq N$$

In the numerical simulation, entropy waves enter the computational domain from the left side. At the right boundary of the computational domain an absorbing boundary condition, specifically, a perfectly matched layer (PML) is imposed. The PML absorbs all the outgoing entropy waves with little reflection. The PML equations in variables T, u, p are:

$$\frac{\partial T}{\partial t} + M \frac{\partial T}{\partial x} + (\gamma - 1) \bar{T} \frac{\partial u}{\partial x} + \sigma(1 + \beta M)T + \sigma\beta(\gamma - 1)\bar{T}u = 0 \quad (9)$$

$$\frac{\partial u}{\partial t} + M \frac{\partial u}{\partial x} + \frac{\bar{T}}{\gamma \bar{p}} \frac{\partial p}{\partial x} + \sigma(1 + \beta M)u + \sigma\beta \frac{\bar{T}}{\gamma \bar{p}} p = 0 \quad (10)$$

$$\frac{\partial p}{\partial t} + M \frac{\partial p}{\partial x} + \gamma \bar{p} \frac{\partial u}{\partial x} + \sigma(1 + \beta M)p + \sigma\beta\gamma \bar{p}u = 0 \quad (11)$$

$$\beta = \frac{M}{\bar{T} - M^2} \quad (12)$$

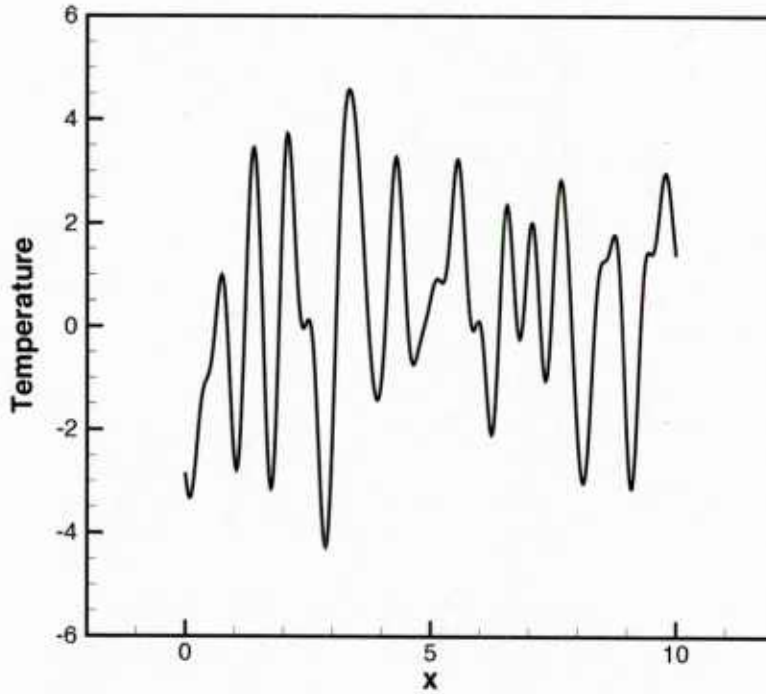


Figure 5. An instantaneous spatial distribution of entropy wave blobs from numerical simulation.

Figure 5 shows an instantaneous spatial distribution of the computed entropy wave inside the computational domain. The temperature fluctuations associated with the entropy wave are random. For the present simulation, the typical blob size is 1.0 as expected. By measuring the temperature fluctuation in the computational domain over a sufficiently long period of time, an autocorrelation function as well as a spectrum can be computed from the measured data. Figure 6 shows a comparison between the measured and the prescribed autocorrelation function. Figure 7 shows the prescribed spectrum. Figure 8 shows the spectrum recovered from the random simulation data. It is evident that the simulation results are in good agreement with the prescribed autocorrelation function and spectrum.

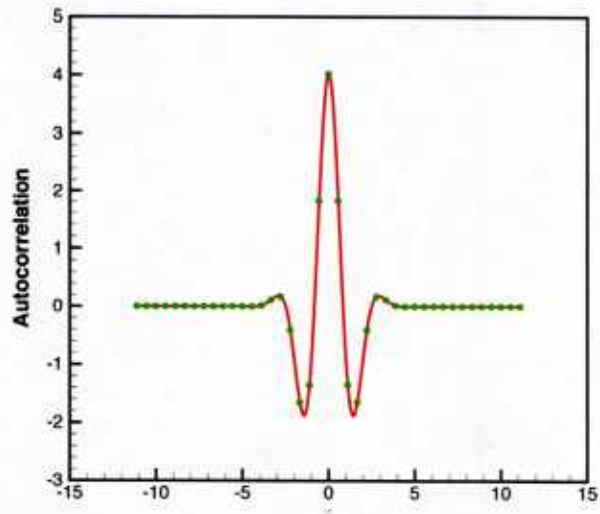


Figure 6. Comparison between prescribed and measured autocorrelation function. Full line is the prescribed and dots is the measured autocorrelation.

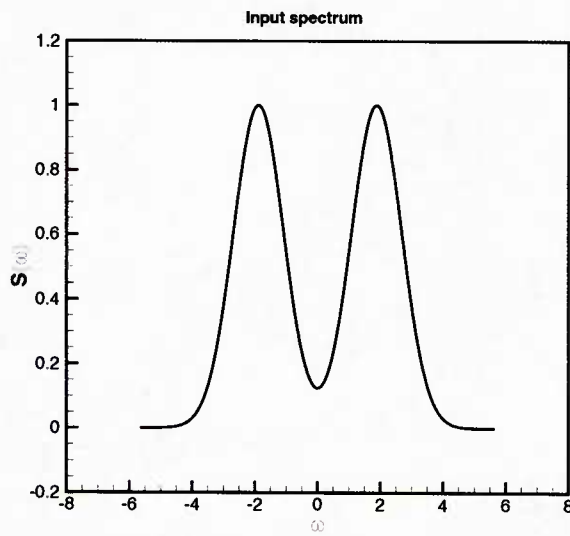


Figure 7. The prescribed spectrum of the random entropy wave field.

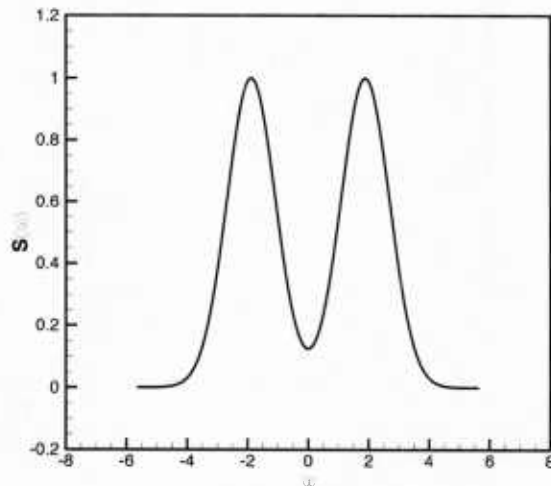


Figure 8. Power spectral density of the random temperature fluctuations associated with the incoming broadband entropy wave field.

Figure 9 shows the two-point cross-correlation of the temperature field of the entropy waves. The dots are the computed results using the measured data (the fixed point is in the center of the computational domain). The full line is the prescribed cross-correlation function of the model boundary condition. The agreement is excellent. The half-width of the cross-correlation function is a good measure of the size of the entropy blobs generated by the model.

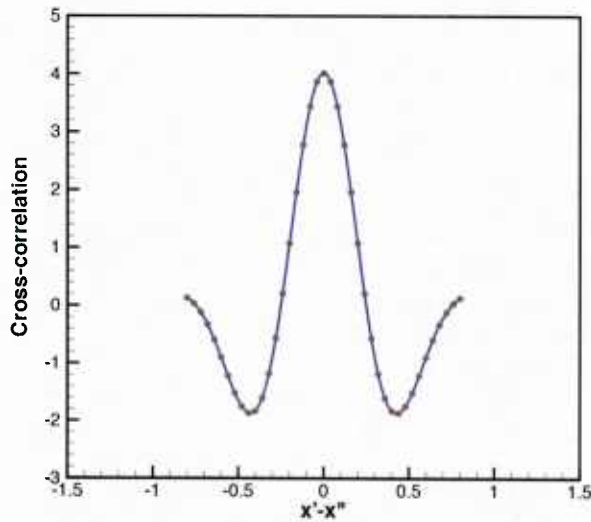


Figure 9. Full line is the input cross-correlation function. Dots are cross-correlation function computed using the measured random data from the simulation.

Currently we are working with Allan Aubert of NAVAIR on analyzing the noise of F18E at different power setting. We expect to report preliminary findings in the next quarterly progress report.